Chapter 10
Parallel Optical and Electrochemical DNA Detection

Wolfgang Knoll, Jianyun Liu, Lifang Niu, Peter Eigil Nielsen, and Louis Tiefenauer

Abstract This contribution introduces strategies for the sensitive detection of oligonucleotides as bio-analytes binding from solution to a variety of probe architectures assembled at the (Au-) sensor surface. Detection principles based on surface plasmon optics and electrochemical techniques are compared. In particular, cyclic- and square wave voltammetry (SWV) are applied for the read-out of ferrocene redox labels conjugated to streptavidin that binds to the (biotinylated) DNA targets after hybridizing to the interfacial probe matrix of either DNA or peptide nucleic acid (PNA) strands. By employing streptavidin modified with fluorophores the identical sensor architecture can be used for the recording of hybridization reactions by surface plasmon fluorescence spectroscopy (SPFS). The Langmuir isotherms determined by both techniques, i.e., by SWV and SPFS, give virtually identical affinity constants K_A, confirming that the mode of detection has no influence on the hybridization reaction. By using semiconducting nanoparticles as luminescence labels that can be tuned in their bandgap energies over a wide range of emission wavelengths surface plasmon fluorescence microscopy allows for the parallel read-out of multiple analyte binding events simultaneously.

W. Knoll (✉)
AIT Austrian Institute of Technology, Donau City Strasse 1, 1220 Vienna, Austria
e-mail: Wolfgang.Knoll@ait.ac.at

J. Liu • L. Niu
Max Planck Institute for Polymer Research, Ackermannweg 10, D-55128 Mainz, Germany

P.E. Nielsen
Department of Biochemistry B, The Panum Institute, IMBG, Blegdamsvej 3c, DK-2200 Copenhagen, Denmark

L. Tiefenauer
Department of Chemistry, Life Sciences Department, Paul Scherrer Institute, CH-5232 Villingen, PSI, Switzerland

G. Spoto and R. Corradini (eds.), *Detection of Non-Amplified Genomic DNA*, Soft and Biological Matter, DOI 10.1007/978-94-007-1226-3_10,

10.1 Introduction

The question as to which detection method – electrical/electrochemical or optical schemes – eventually will win the race for the most powerful transducer principle in bio-sensing is still completely open. The option for higher integration density on chips or in any other array format and the ease of coupling the output signals directly to data analysis electronics certainly points to electrical detection schemes, however, optics is still leading in terms of sensitivity: fluorescence spectroscopy and, in particular, single photon detection are routine methods with unmatched detection limits while the well established electrochemical techniques do not allow for the monitoring of such extremely low currents. And single electron (transistor) recordings are yet to be combined with the aqueous environment needed for bio-affinity studies [1].

A very reasonable experimental approach to further tackle this question is the parallel use of an optical scheme and an electrochemical technique for the simultaneous recording of binding events of bio-analytes from solution to interaction partners covalently attached to the sensor surface via functional architectures assembled at the transducer/analyte solution interface. Surface plasmon resonance spectroscopy [2] and cyclic or differential pulse voltammetry [3] are very well suited for such a combination approach: the (noble) metal substrate needed for the resonant excitation of a propagating surface plasmon mode at the metal/buffer interface can be simultaneously used as the working electrode of a regular three electrode electrochemical set-up. This way, bio-affinity studies can be performed with both techniques in parallel.

A certain limitation to this approach, however, is given by the need to design and assemble the interfacial layer deposited at the sensor surface for an optimized performance of the respective transduction principle. We will demonstrate this for a series of hybridization studies between surface-attached oligonucleotide catcher probes and their (fully complementary or mismatched) target sequences from solution. These target analytes were labeled with streptavidin that was either derivatized with ferrocene for the electrochemical detection or with a chromophore suitable for surface plasmon fluorescence spectroscopic investigations [4].

The use of semiconducting nanoparticles, quantum dots, offers interesting aspects for both schemes: The tunability of the emission wavelength via bandgap engineering of the quantum dots allows for multiple parallel recording of simultaneous binding events on an array sensor by color multiplexing [5]. On the other hand, the manipulation of the energy level of the substrate (by applying an electrical potential) and, hence, the electronic interaction between substrate and nanoparticles – covalently ‘wired’ to the (Au-) electrode – promises interesting coupling schemes [6] and the use of the observed new photo-electrochemical phenomena for completely unconventional biosensor recording principles1.

10.2 Experimental Apparatus

A schematic of the employed combination set-up is given in Fig. 10.1a. The basic instrument is a classical surface plasmon resonance (SPR) spectrometer in the Kretschmann configuration. The thin Au layer evaporated onto the base of the coupling prism is used simultaneously as the active metal/dielectric interface that guides the evanescent surface plasmon mode and can be employed as the working electrode in a typical electrochemical set-up. The two common modes of operation in SPR – the angular scans and the time-dependent kinetic recordings at a fixed angle of incidence – are schematically given in Fig. 10.1b, c, respectively. By attaching, in addition to the working electrode, also a counter and reference electrode to the flow

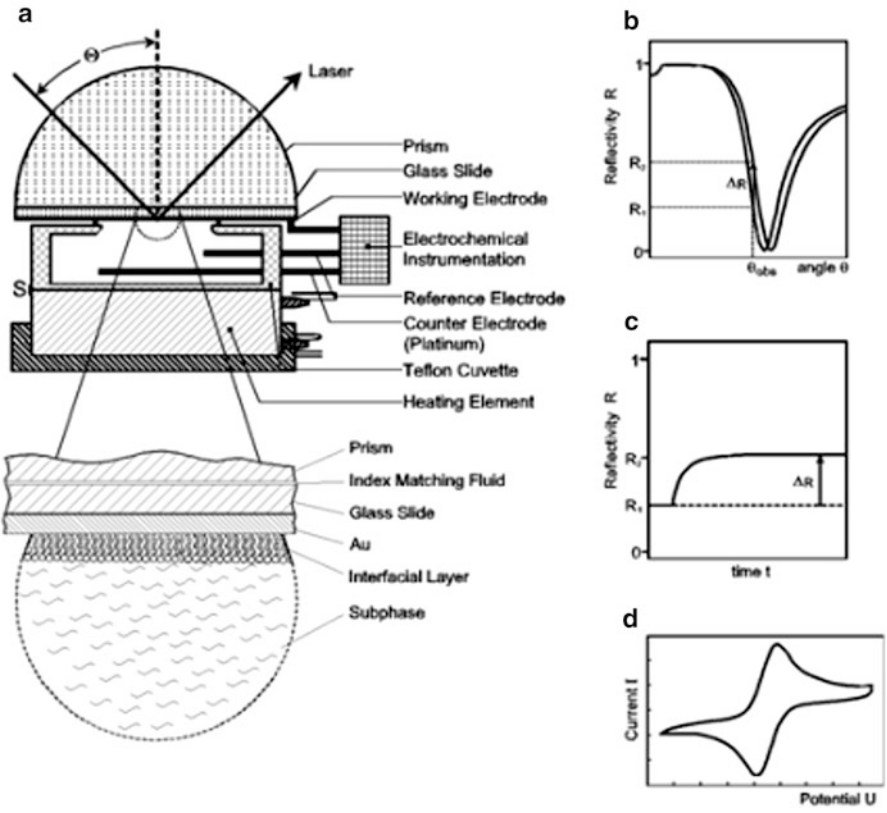

Fig. 10.1 (**a**) Schematic of a surface plasmon spectrometer in the prism-coupled Kretschmann configuration in combination with electrochemical instrumentation; (**b**) angular scan SPR measurements before (*left curve*) and after a thin film deposition, e.g., a layer of capture probes assembled (*right curve*); (**c**) kinetic SPR measurement taken as a function of time at a fixed angle of incidence (and observation), cf. (b); (**d**) schematic of a cyclic voltammogram taken by the electrochemical set-up coupled to the SPR instrument

cell, classical electrochemical techniques, e.g., cyclic voltammetry (cf. Fig. 10.1d), square wave voltammetry (SWV), or impedance spectroscopies [3] can be employed for the functional characterization of interfacial architectures.

A further extension of this combination set-up will be presented in Fig. 10.8: a fluorescence detection unit is attached in a way that the photons emitted by chromophores that are sufficiently close to the interface to be excited by the surface plasmon modes can be detected either as a function of the angle of incidence (tuning the resonance) or as a function of time for kinetic recordings [7].

Depending on whether electrochemical or surface plasmon optical measurements are to be performed the interfacial architectures assembled at the sensor surface need to fulfil different requirements: in order to optimize the electron transfer from a redox label to the electrode that is – in one way or another – the basis for electrochemical biosensing the redox-active unit has to be wired to the electrode interface in a most efficient way. The assembly of the sensor coating that were used for surface hybridization studies is schematically given in Fig. 10.2: onto the bare Au substrate a binary mixture of thiolated PNA oligonucleotides (i.e., the synthetic mimics of natural oligonucleotides with a neutral pseudo-peptide backbone [8]) of a particular sequence (HS-PNA) are co-adsorbed with a diluent molecule, mercaptohexanol (MCH), that optimizes the lateral packing of the probe oligonucleotides for the hybridization reactions (Fig. 10.2a). After hybridization of biotinylated target strands from solution to the probe matrix at the sensor surface (Fig. 10.2b), the biotin groups are 'decorated' in a 1:1 stoichiometric ratio by streptavidin molecules that carry a number of ferrocene molecules covalently attached to the protein through a spacer (Fig. 10.2c). A schematic of the protein structure and one ferrocene spacer unit are given in Fig. 10.2d.

Table 10.1 summarizes details of the employed molecular structures and the specific sequences of probe and target PNAs and DNAs [9]. In addition to the probe HS-PNA-P1 with a 15-mer recognition sequence coupled via the spacer groups to the thiol unit for the linking to the Au substrate the equivalent DNA analogue with the same recognition sequence P1, however, with a spacer unit of 15 thymines and a biotin anchor that allows the molecule to be assembled onto a streptavidin monolayer employed in the optical experiments as a generic binding matrix (cf. also Fig. 10.10) was used. For studies on mismatch discrimination another probe DNA, i.e., the biotin-DNA-P2 was used. This recognition sequence differs by a single base (underlined and in *italics* in Table 10.1).

The target strands follow two different molecular construction principles: for the electrochemical detection the DNA targets used are all modified with a biotin group at the 5′ end. This will allow for the coupling of the ferrocene-labeled streptavidin as redox-markers after hybridization (cf. the scheme given in Fig. 10.2b, c). For the surface plasmon fluorescence spectroscopic experiments the targets in one case were also modified with a biotin which after hybridization, however, were detected via the binding of a fluorophore-labeled streptavidin molecule. For the color multiplexing experiments QDs emitting at different wavelengths (cf. Table 10.1) were directly coupled to the various targets.

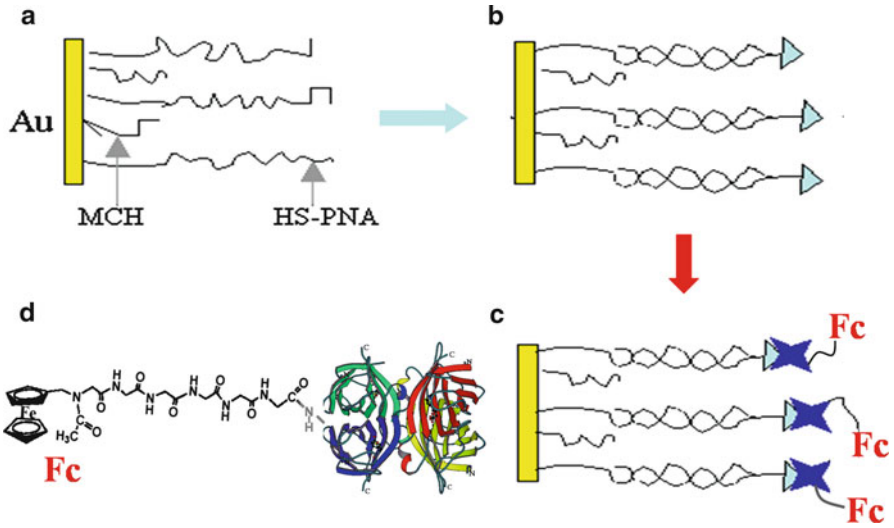

Fig. 10.2 Interfacial architecture self-assembled at the sensor surface for electrochemical read-out of hybridization reactions: (**a**) onto the Au substrate used for SPR- and electrochemical measurements a binary mixture of thiolated PNA strands and mercaptohexanol (MCH) as diluent molecules are forming a functional monolayer; (**b**) after hybridization with biotinylated target strands resulting in DNA duplex formation, ferrocene-labeled streptavidin can be bound to the surface layer (**c**). Some structural details of the ferrocene-labeled streptavidin Fc-Stv are shown in (**d**). Typically, 9 ferrocenes are attached to one streptavidin resulting in a corresponding amplification of the binding signal

Table 10.1 Probe and target sequences used in the experiments

Name	Nucleotide sequence
Probes	
HS-PNA - P1	Cys-[eg1]$_6$ - TGT ACA TCA CAA CTA - NH2
	Cys-[eg1]$_6$: 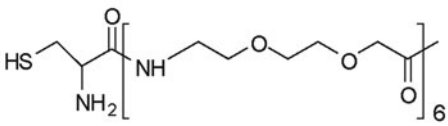
Biotin - DNA - P1	5'-biotin - $(TTT)_5$ - TGT ACA TCA CAA CTA - 3'
Biotin - DNA - P2	5'-biotin - $(TTT)_5$ - TGT AC*G* TCA CAA CTA - 3'
Targets	
T1 - biotin	3' - ACA TGT AGT GTT GAT - biotin - 5'
T1 - QD_{565}	3' - ACA TGT AGT GTT GAT - **QD_{565}** - 5'
T2 - QD_{655}	3' - ACA TG<u>C</u> AGT GTT GAT - **QD_{655}** - 5'

10.3 Electrochemical Sensing of Hybridization Reactions

The combination of the electrochemical cell with a surface plasmon spectrometer allows for the structural characterization of the sequential assembly of the interfacial architecture by surface plasmon optical (angular and/or time-dependent) scans followed by the functional assessment of the resulting sensor surface coating by, e.g., cyclic voltammetry. This is documented in Figs. 10.3 and 10.4, respectively, for surface architectures based on the assembly of thiolated molecules directly onto the Au substrate. This results in the formation of a functional monolayer exposing a specific nucleotide sequence to the target strands injected subsequently into the sample cell. The minute shift of the SPR resonance curve upon binding of the targets to the surface probe layer (cf. Fig. 10.3, dots to solid curve) indicates the limited sensitivity of SPR in this case of a small analyte molecule (small molecular mass compared to a typical protein) bound to the surface at a moderate surface density. Only upon decoration of the hybrid monolayer with a layer of streptavidin bound via the target-attached biotin-groups results in a significant shift of the SPR angular scan curve that could be used for a more quantitative analysis of the affinity of this hybridization reaction. Effectively, the streptavidin acts as a mass label in SPR detection. From the angular shift of $\Delta\theta = 0.25°$ one calculates a thickness of the streptavidin layer of c. $\Delta d = 2.1$ nm (assuming a refractive index of $n = 1.45$), corresponding to a protein density of about $1.3 \cdot 10^{12}$ cm^{-2}.

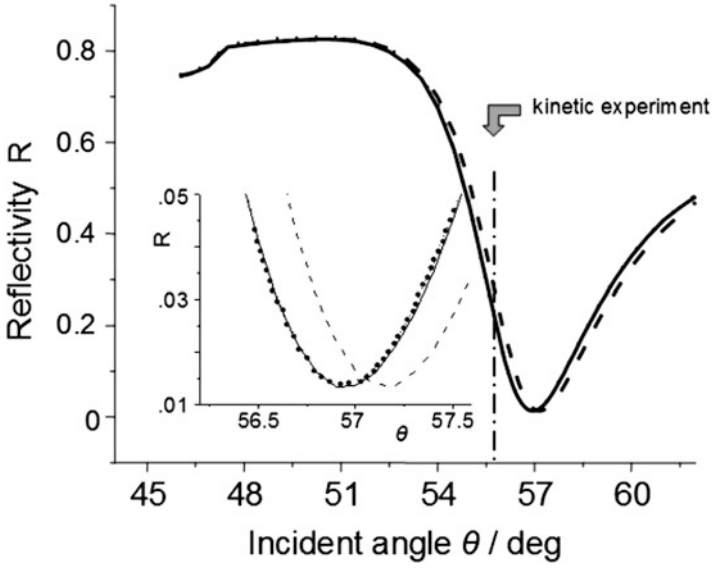

Fig. 10.3 SPR curves recorded in 20 mM PB buffer with 0.005% Tween 20 after PNA/MCH immobilization (*dots*), after hybridization with 500 nM target (*solid curve*) and after Fc-Stv adsorption (200 nM, *dashed curve*). The *inset* is an expanded view of the SPR minima part

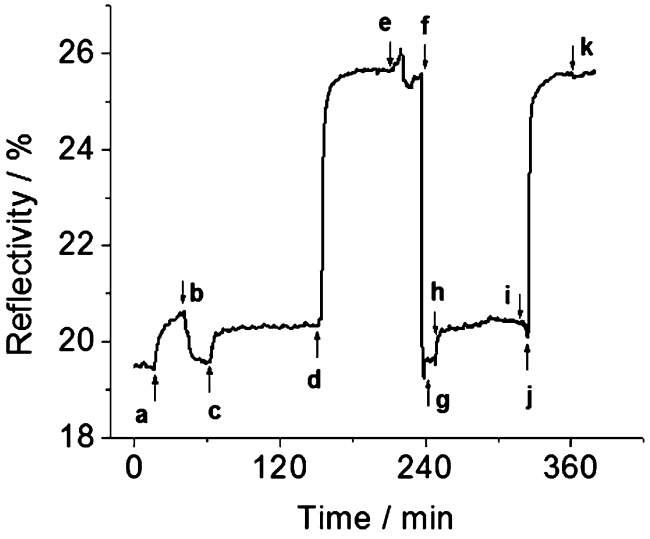

Fig. 10.4 SPR kinetic curve measured at a fixed incident angle ($\theta = 55.7^{o}$): (*a*) injection of 200 nM Fc-Stv after rinsing a 1 μM non-complementary biotinylated target solution through the cell; (*b*) rinsing with buffer; (*c*) injection of 500 nM fully complementary biotinylated target; (*d*) after rinsing and then injection of 200 nM Fc-Stv; (*e*) rinsing with buffer; (*f*) rinsing with 50 mM NaOH in order to regenerate the probe matrix; (*g*)–(*k*) repeating the steps (*b*)–(*e*)

The equivalent kinetic experiment and a few more reference scans are shown in Fig. 10.4. After assembling the probe matrix and injecting an analyte solution with fully mismatched target strands (a), rinsing with neat buffer results in the complete return of the reflected intensity at this fixed angle of observation to the reference level (b). Injection of the complementary, biotinylated target results in a small increase of the reflectivity (c) which – upon injection and binding of the ferrocene-labeled streptavidin (Fc-Stv) – shows the strongly amplified reflectivity increase expected from the angular scans displayed in Fig. 10.3 (d). Regeneration of the probe matrix by injecting a 50 mM NaOH solution through the flow cell (f) results in the return of the reflected intensity to the level measured prior to any hybridization. This observation and the displayed fully repeatable hybridization, i.e., association/dissociation (regeneration) cycle added in Fig. 10.4 indicates the excellent control over the supramolecular functional architecture and the stability of the attached components upon repeated hybridization cycles (Fig. 10.4g–k).

Figure 10.5 shows a series of cyclic voltammograms taken with a sample that was prepared by hybridizing the fully matched target T1-biotin from a 500 nM solution to the surface-bound probe matrix and decorating the hybrids by a monolayer of Fc-Stv [10]. The flexibility of the double strand and the six glycine residues of the linker used to couple the ferrocene to the streptavidin allow for a rather effective electron transfer from the redox site to the electrode and *vice-versa*. The CV curves recorded at different scan rates are perfectly symmetrical, indicating a fully reversible electron transfer reaction. The peak currents are proportional to

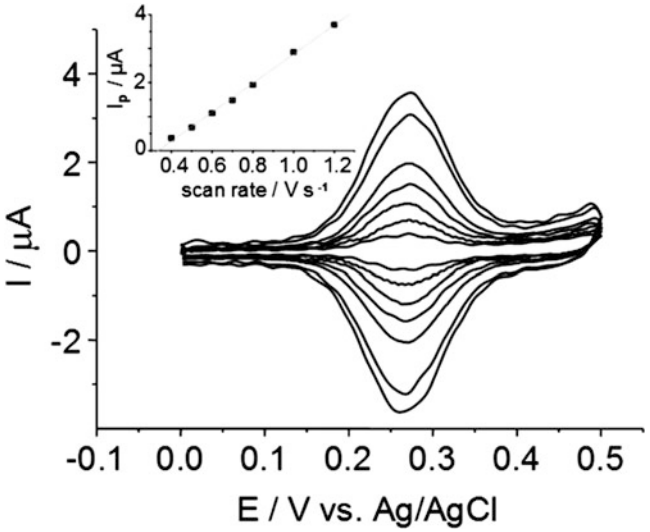

Fig. 10.5 Cyclic voltammograms of Au/PNA/fully complementary target/Fc-Stv measured in buffer with different scan rates, i.e., 0.4, 0.5, 0.6, 0.7, 0.8, 1.0 and 1.2 V/s from inside to outside, respectively. The *inset* shows the linear relationship between peak currents and scan rates

the scan rates, confirming a surface-controlled redox reaction only (cf. the insert in Fig. 10.5). The slightly broadened peak width (i.e. 120 mV compared to the ideal value of 90.6 mV for a reversible one electron surface transfer reaction) possibly indicates some ferrocene interactions and a random distribution of the redox labels within the film. Assuming that one biotinylated target can bind one streptavidin and that all Fc sites are electroactive the amount of bound DNA target can be calculated by integrating the current under the anodic (or cathodic) charge transfer wave in the CV. The obtained value of $\Gamma = 1.1 \cdot 10^{12}$ cm^{-2} corresponds well to the value obtained by SPR ($1.3 \cdot 10^{12}$ cm^{-2}, see above), indicating that, indeed, most of the ferrocenes are electroactive.

The number of bound DNA molecules, hybridized to the PNA matrix depends on the target concentration in the bulk solution, c_0. In particular, at low concentration only a fraction of the maximum PNA/DNA duplexes at the interface can be formed. With increasing concentration of c_0 more and more hybrids are formed until eventually a complete monolayer is asymptotically reached. Within the Langmuir model which requires certain conditions to be met, e.g., that all binding sites are equivalent and that the association and dissociation rate constants do not depend on the coverage, a simple relation for the coverage, Γ, at the sensor surface and the bulk concentration c_0 holds:

$$\theta = K_A c_0 / (1 + K_A c_0) \tag{10.1}$$

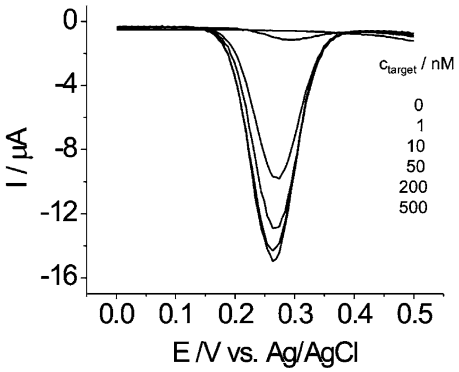

Fig. 10.6 Square wave voltammograms taken after the hybridization reactions of surface-grafted PNA oligonucleotide strands (cf. Fig. 10.2a) and fully complementary biotinylated target strands of different concentrations, as indicated, after Fc-Stv binding to saturation. Frequency: 100 Hz, amplitude: 20 mV

where θ is the fractional coverage defined as $\theta = \Gamma/\Gamma_{max}$ and Γ_{max} is the maximum coverage given by the number density of PNA probe strands at the sensor surface.

With the sensor architecture presented in Fig. 10.2 we can assume that one biotinylated target strand is able to bind to one Fc-labeled streptavidin molecule. Hence, the recorded current should be proportional to the DNA target coverage and will allow for the determination of the affinity constant K_A:

$$I(c_0) = I_m K_A c_0 / (1 + K_A c_0) \tag{10.2}$$

Figure 10.6 displays a series of SWV curves taken after Fc-Stv was bound to the biotinylated target strands after they hybridized to the sensor matrix from bulk solutions of different concentrations, as indicated. Clearly, with increasing target concentration the corresponding redox peak currents increase. If these peak currents are plotted as a function of the bulk target concentration c_0, the saturation behavior is found (cf. Fig. 10.7, (-◇-)) as expected from the Langmuir model that has been demonstrated by optical techniques to describe this process at the sensor interface very well. If fitted to the Langmuir model according to Eq. 10.2, an affinity constant of $K_A = 1.5 \cdot 10^8\ M^{-1}$ is found (Fig. 10.7, blue curve). This value agrees well with other reports based, e.g., on the use fluorescently labeled targets, in particular, if differences in the interfacial architecture, i.e., the coupling chemistry, the spacer length, the probe density, etc., are taken into account.

10.4 Fluorescence Spectroscopic Sensing of Hybridization Reactions

As it has been introduced recently, fluorescence detection schemes in combination with the optical field enhancement mechanisms operating at resonant surface plasmon excitation result in significant sensitivity gains for biosensing applications: for proteins binding to a quasi-3D matrix a limit of detection (LOD) of

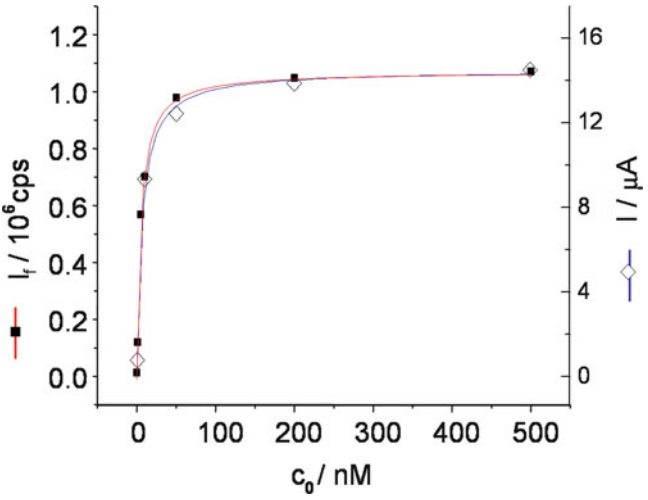

Fig. 10.7 Langmuir isotherms of PNA/DNA hybridization constructed from the electrochemical data presented in Fig. 10.6 (-◇-) and from the surface plasmon fluorescence data shown in Fig. 10.9 (-■-) and fitting curves (*red* for SPFS data, *blue* for electrochemical data)

$c_0 = 500$ aM [11], and for PCR hybridization to a 2D probe layer a LOD of $c_0 = 100$ fM [8] have been reported. As mentioned before the attachment to a regular SPR set-up required for surface plasmon fluorescence spectroscopy (SPFS) is rather trivial: a lens in front of the metal-coated prism base that guides the surface plasmon wave collects the fluorescence photons emitted from chromophores that are within the range of the evanescent surface mode. After passing an attenuator (in order to restrict the count rates to the linear response range of the detector) and a bandpass filter (for discrimination of the fluorescence emission against merely scattered light) this photoluminescence is then recorded by a photomultiplier tube or – in case of the microscopic mode of operation (cf. below) – by a color CCD camera. The whole arrangement is mounted to the SPR instrument in such a way that it rotates in the angular mode with the prism thus recording fluorescence photons emitted normal to the interface. The scheme of this instrumental setup is given in Fig. 10.8.

The possibility to employ fluorescently-labeled streptavidin (Fluor-Stv) (instead of the ferrocene-labeled analogue) for the decoration of surface-hybridized biotinylated target strands allows for a direct comparison of SPFC data with the electrochemical results presented in Figs. 10.6 and 10.7, respectively [10]. To this end, a series of angular SPFS curves were recorded after hybridization of targets from solutions of different concentrations and after the binding of Fluor-Stv. The results are summarized in Fig. 10.9. Similar to the current in the case of the SWV scans, here, the fluorescence intensity increases as one increases the bulk concentration of the target solutions, c_0. Note the slight shift of the angular peak position of the maximum intensity (which is also reflected in the slight shift of the position of the reflectivity minima) upon the increase in surface coverage of the

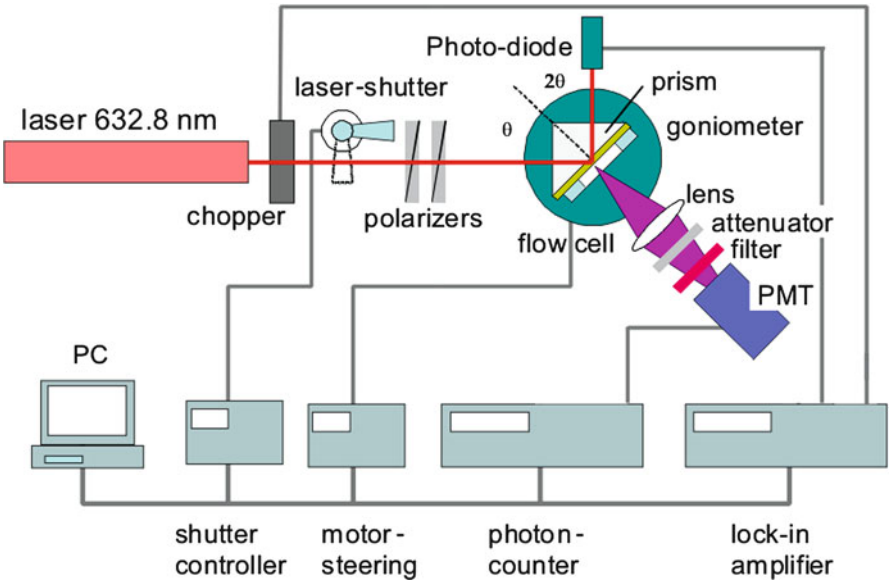

Fig. 10.8 Schematics of a surface plasmon fluorescence spectrometer, based on a normal SPR instrument with an attached fluorescence detection module. A photomultiplier tube (*PMT*) is used as the detector in the spectroscopic mode; however, in the imaging mode (cf. Fig. 10.11) a color CCD camera can be attached

bound streptavidin. Similar to the peak currents of the SWV scans the plot of the peak fluorescence intensities as a function of c_0 (cf. Fig. 10.7, -■-) shows the typical Langmuir isotherm behavior with the saturation at higher concentration (Fig.10.7, blue curve).

As one can see by the almost perfect superposition of the SWV and the SPFS data both methods give nearly identical K_A-values and, hence, confirm that both methods detecting their respective, yet very similar labels (Fc-Stv vs. Fluor-Stv) and the quantitative analysis of the data is not affected methodologically. As far as the sensitivity of the two techniques is concerned one should also expect similar limits of detection because the S/N levels in both data sets are rather equivalent (cf. Figs. 10.6 and 10.9).

The general interest in sensor platforms that allow for the parallel detection of multiple binding events typically requires a chip format in which the individually sensing elements functionalized for a particular analyte are arranged in an array matrix [12]. Read-out can then be achieved either in a serial manner (e.g., by a fluorescence scanner) or in a parallel way by a (microscopic) imaging mode [13].

The use of semiconducting nanoparticles, quantum dots (QDs), offers an alternative approach based on the possibility to engineer their emission wavelength by size (quantum confinement) or compositional control of their bandgap energy [14]. This way, very similar labels that all can be excited by the same laser wavelength

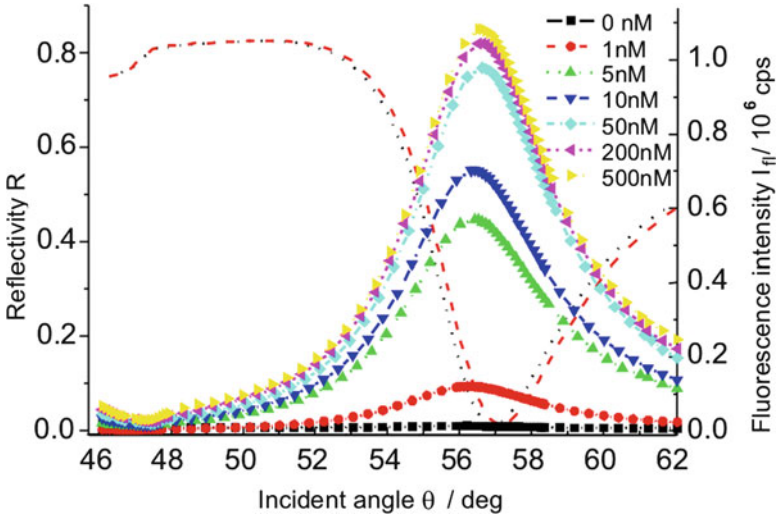

Fig. 10.9 A series of angular reflectivity (*dotted* and *dashed*) curves and SPFS scans (*curves* with *symbols*) taken after the hybridization of biotinylated, fully complementary target strands from solutions of different concentrations and the decoration of the duplex layer by fluorophore-derivatized streptavidin (*Fluor-Stv*). Note the slight shift of the angular peak position due to the increasing surface density of bound streptavidin; *dotted curve*: before hybridization, *dashed curve*: after hybridization with 500 nM target followed by binding of Fluor-Stv

but which emit in different luminescence colors can be synthesized and attached to the respective bio-analytes. Color multiplexing thus allows for the simultaneous recording of the binding signals of a whole set of analyte molecules in a mixture [5].

This concept and its implementation for surface hybridization studies is schematically given in Fig. 10.10. Here, the initial concept for the functional assembly of the sensor coating is modified by first assembling a monolayer of a binary mixture of 10% of a biotinylated thiol derivative laterally diluted by 90% of mercaptohexanol. Onto this coating a streptavidin monolayer as a generic binding matrix is assembled to which other biotinylated units can be attached, e.g., different oligonucleotide probe strands. Their base sequences are complementary to different DNA targets in the analyte solution which, in turn, are coded on different colors by carrying QDs of different emission wavelengths. Their simultaneous recording after hybridization allows for a multiple detection of a variety of analytes in parallel.

An example along this concept is demonstrated in Fig. 10.11. The flow cell was equipped with four Au electrodes that could be used as SPR/SPFS substrates [15]. After the general assembly of a protective coating to all electrodes (i.e., a poly (ethylene oxide) thiol SAM (PEO-SAM)) the flow cell was mounted to the spectrometer. The individual potential control of the four electrodes could then be used for the sequential functionalization of each Au area separately. Firstly, one of the electrodes was subject to a cathodic scan thus reductively desorbing its PEO-SAM, generating a bare, clean Au surface. Injecting sequentially (i) the binary

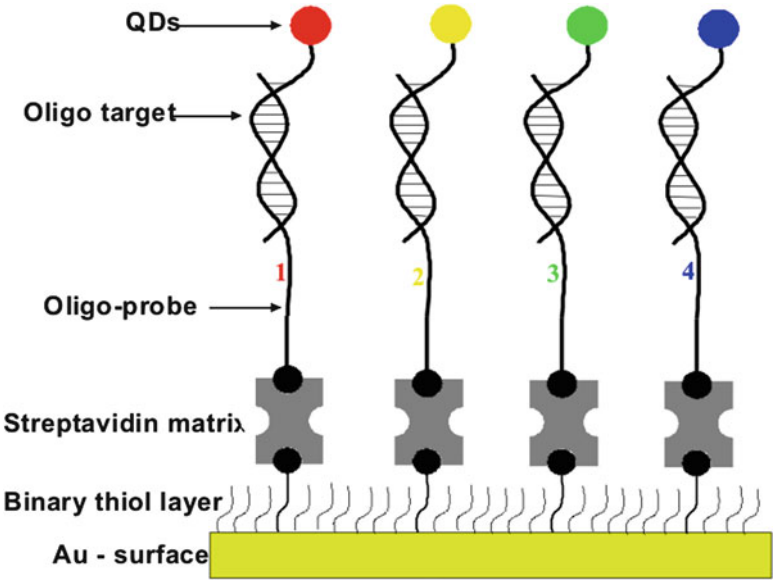

Fig. 10.10 Interfacial architecture optimized for multiple parallel surface hybridization studies in the color multiplexing mode with semiconducting nanoparticles emitting fluorescence light at different wavelengths: Onto the Au substrate a binary monolayer of biotinylated thiols mixed with OH-terminated thiols as diluent molecules is self-assembled, followed by the binding of a monolayer of streptavidin. To this generic binding matrix a mixture of different biotinylated probe oligonucleotides are assembled. They can specifically hybridize to their respective complementary target strands which are sequence-coded by quantum dots of different colors

(biotin-/OH-) thiol mixture, (ii) streptavidin and then (iii) a specific biotinylated PNA oligonucleotide solution (e.g., the Biotin-DNA-T1, cf. Table 10.1) results in the selective functionalization of this electrode only, while the other ones still remain protected by their PEO-SAM. By a step-and-repeat procedure eventually all electrodes are functionalized with no cross-contamination from one area to the neighboring electrode.

This way, the electrode array in Fig. 10.11 was functionalized with Biotin-DNA-P1 (P1), Biotin-DNA-P2 (P2), a mixture of both probes for the color multiplexing experiment, and a PEO-SAM used as an inert reference (cf. Fig.10.11a).

After injection of a 200 nM solution of the T2 target, coded with QDs emitting at $\lambda = 655$ nm, the surface plasmon fluorescence microscopic image displays the expected red color on the second and forth electrode (from top to bottom, cf. Fig. 10.11b) that both expose to the analyte solution the probe strand P2 which is fully complementary to T2 (cf. Table 10.1). The third electrode shows only a very faint reddish color corresponding to only a minute surface binding according to the significantly reduced affinity for T2 hybridizing to P1 which represents a mismatch 1 (MM1) situation with an affinity constant about two orders of magnitude lower than MM0. The reference electrode covered with the PEO-SAM remains completely dark.

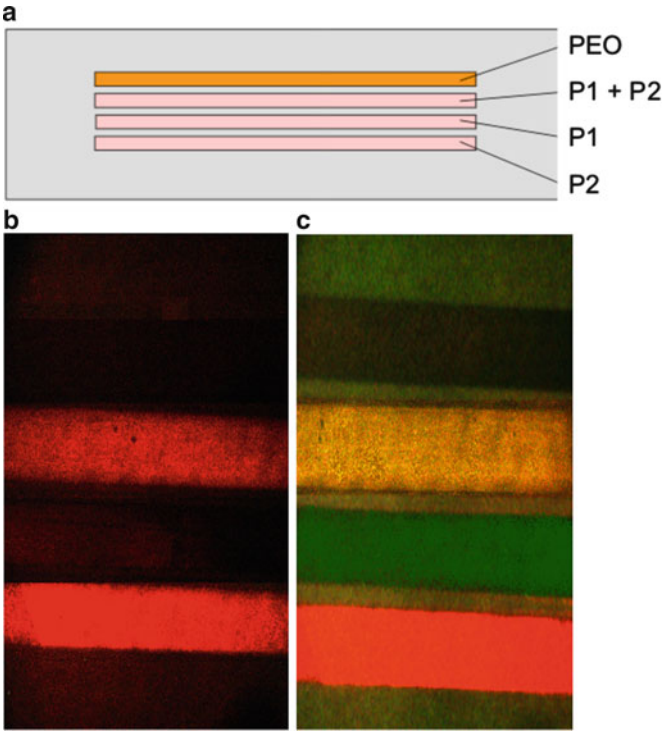

Fig. 10.11 Surface plasmon fluorescence microscopy: (**a**) Schematic arrangement (*top view*) of the probe oligonucleotides P1 and P2 and a mixture of both, as indicated, on a four-electrode chip for hybridization studies with target oligonucleotide strands labeled with quantum dots; (**b**) SPFM image showing the *red color* emitted after the hybridization of the target T2 which is complementary to P2 and is carrying a QD emitting at $\lambda = 655$ nm; (**c**) SPFM taken after the hybridization of a second injected target sequence T1, fully complementary to P1 and coded with a QD emitting at $\lambda = 565$ nm. Note the (artificial) mixture of *red* and *green* in the CCD camera to result in a *yellow color*

After rinsing and injecting the T1 solution the result shown in Fig. 10.11c is obtained after the hybridization reaction was completed. The third electrode exposing the MM0 probe P1 turns green corresponding to the binding of the targets T1 with their QDs emitting at $\lambda = 565$ nm. The forth electrode remains red (the emission appears to be more intense only because the integration time was increased in order to account for the lower quantum yield of the green emitting QDs), while the PEO-SAM also in this case appears to be completely inert.

The second electrode area now looks yellow. However, this is only a (well-known) artefact of the color CCD camera that mixes red and green to yellow. The same result was obtained upon the injection of a solution mixture of the target analytes rather than their sequential injection. Analysing the emitted light via a spectrometer clearly demonstrates that only light originating from green and red

emitting QDs is recorded. This experiment demonstrates that color multiplexing is an option for multiple analyte sensing; however, it requires the spectral analysis by a spectrometer for the unambiguous identification of the emitted colors.

10.5 Conclusions

The presented results document that both, fluorescence-optical and electrochemical principles, are well suited to monitor bio-analyte binding from the aqueous phase to specific functional sites assembled at the sensor surface. Although the read-out of redox labels doesn't quite reach the sensitivity of fluorescence recordings electrochemical techniques offer the advantage of giving direct electrical signals that can be used for data analysis.

Very attractive for both methods are semiconducting nanoparticles. The possibility of tuning their emission wavelength makes them very attractive labels in photoluminescence studies, e.g., for color multiplexing in parallel schemes for multiple analyte detection. One must bear in mind, however, that complications arise from the still unsolved problem of the luminescence blinking of QDs [16].

Particularly promising are schemes that couple the electronic orbitals of QDs to the Fermi-level of the metallic substrate. This way a completely new principle for the interplay between QDs as light emitting fluorophores and their electron donating or accepting properties are conceivable and should give rise to novel ways for the sensitive detection of bio-analyte binding [17].

Acknowledgments Partial funding for this project from the Deutsche Forschungsgemeinschaft (DFG, KN 224/13-1 and 13-2, and SFB 625) is gratefully acknowledged. We thank Thomas Basché, Ming-Yong Han, and Shengjun Tian for many helpful discussions.

References

1. Kastner, M.A.: The single electron transistor and artificial atoms. Ann. Phys. **9**, 885–894 (2000)
2. Knoll, W.: Interfaces and thin films as seen by bound electromagnetic waves. Annu. Rev. Phys. Chem. **49**, 569–638 (1998)
3. Kaifer, A.E., Gómez-Kaifer, M.: Supramolecular Electrochemistry. Wiley- VCH, Weinheim (2001)
4. Liebermann, T., Knoll, W.: Colloids and Surfaces A **171**, 115–130 (2000)
5. Robelek, R., Niu, L., Schmid, E., Knoll, W.: Multiplexed hybridization detection of quantum Dot conjugated DNA sequences using surface Plasmon enhanced fluorescence microscopy and spectrometry. Anal. Chem. **15**, 6160–6165 (2004)
6. Cameron, P.J., Zhong, X., Knoll, W.: Electrochemically controlled surface Plasmon enhanced fluorescence response of surface immobilized CdZnSe quantum dots. J. Phys. Chem. C **113**, 6003–6008 (2009)
7. Knoll, W., Yu, F., Neumann, T., Niu, L., Schmid, E.: Principles and applications of surface-plasmon field- enhanced fluorescence techniques. In: Lakowicz, J.R., Geddes, C.D. (eds.) Topics in Fluorescence Spectroscopy. Vol 8: Radiative Decay Engineering, pp. 305–332. Springer, Berlin/Heidelberg/New York (2005)

8. Yao, D., Yu, F., Kim, J., Scholz, J., Nielsen, P., Sinner, E.K., Knoll, W.: Surface plasmon field-enhanced fluorescence spectroscopy in PCR product analysis by peptide nucleic acid probes. Nucleic Acids Res. **32**, 177–192 (2004)
9. Liu, J., Tian, S., Tiefenauer, L., Nielsen, P., Knoll, W.: Simultaneously amplified electrochemical and surface plasmon resonance optical detection of DNA hybridization based on ferrocene-streptavidin conjugates. Anal. Chem. **77**, 2756–2761 (2005)
10. Liu, J., Tian, S., Tiefenauer, L., Nielsen, P., Knoll, W.: PNA-DNA hybridization study using labeled-streptavidin by voltammetry and surface plasmon fluorescence spectroscopy. Anal. Chem. **78**, 470–476 (2006)
11. Yu, F., Persson, B., Lofas, S., Knoll, W.: Attomolar sensitivity in bioassays based on surface plasmon fluorescence spectroscopy. J. Am. Chem. Soc. **126**, 8902–8903 (2004)
12. Zizlsperger, M., Knoll, W.: Multispot parallel on-line monitoring of interfacial binding reactions by surface plasmon microscopy. Prog. Colloid Polym. Sci. **109**, 244–253 (1998)
13. Liebermann, T., Knoll, W.: Parallel multispot detection of target hybridization to surface-bound probe oligonucleotides of different base mismatch by surface-plasmon field-enhanced fluorescence microscopy. Langmuir **19**, 1567–1572 (2003)
14. Zhong, X., Xie, R., Zhang, Y., Basché, T., Knoll, W.: High-quality violet- to red-emitting ZnSe/CdSe core/shell nanocrystals. Chem. Mater. **17**, 4038–4042 (2005)
15. Niu, L., Knoll, W.: Electrochemically addressable functionalization and parallel readout of a DNA biosensor array. Anal. Chem. **79**, 2695–2702 (2007)
16. Robelek, R., Stefani, F.D., Knoll, W.: Oligonucleotide hybridization monitored by surface plasmon enhanced fluorescence spectroscopy with bio-conjugated core/shell quantum dots. Influence of luminescence blinking. Phys. Status Solid A **203**, 3468–3475 (2006)
17. Sinner, E.-K., Ritz, S., Wang, Y., Dostalek, J., Jonas, U., Knoll, W.: Molecularly controlled functional architectures at biointerfaces. Mater. Today **13**, 46–55 (2010)